Convective invigoration traced to warm-rain microphysics

Xin Rong Chua[1*], **Yi Ming**[1,2]

[1]Program in Atmospheric and Oceanic Sciences, Princeton University, Princeton, New Jersey, USA

[2]Geophysical Fluid Dynamics Laboratory, Princeton, New Jersey, USA

Key Points:

- Higher cloud droplet number concentration increases convective mass flux
- The mechanism involves a vertical cooling-above-warming dipole favorable to convection
- The pattern is caused by enhanced cloud water re-evaporation balanced by more condensation

*Current affiliation: Centre for Climate Research Singapore, Singapore

Corresponding author: Xin Rong Chua, CHUA_Xin_Rong@nea.gov.sg

Abstract

Aerosols are postulated to alter moist convection by increasing cloud droplet number concentration (N_d). Cloud-resolving model simulations of radiative-convective equilibrium show that increased N_d leads to higher convective mass flux, seemingly in line with a popular hypothesis which links the convective invigoration to delayed rain formation allowing more cloud liquid water to be frozen. Yet, the same phenomenon is also present in an alternative model configuration with only warm-rain microphysics, suggesting that one does not have to invoke ice microphysics. The key mechanism lies in the different vertical distributions of the increases in cloud liquid re-evaporation and in water vapor condensation, causing a dipole pattern that favors convection. This is further supported by a mechanism-denial experiment in which weakened cloud re-evaporation tends to mute invigoration. This work represents a major advancement of the process-level understanding of aerosol effects on convection.

Plain Language Summary

Aerosols are thought to alter moist convection by increasing cloud droplet number concentration. According to a popular hypothesis, increased droplet number concentration would delay rain formation, allowing more cloud water to reach the freezing level. The additional latent heating from freezing is presumed to be the cause of stronger convection. We test this hypothesis with a numerical model capable of simulating moist convection, and find that convective invigoration occurs even in the absence of ice processes. A detailed analysis suggests that delayed rain formation increases cloud water re-evaporation. The resulting cooling is balanced primarily by more water vapor condensation. This creates a vertical cooling-above-warming dipole favorable to convection. This work represents a major advancement of the process-level understanding of aerosol effects on convection.

1 Introduction

Atmospheric aerosols play a significant role in influencing convection and precipitation. Aerosols alter Earth's radiative budget through the absorption and scattering of radiation, as well as by altering the albedo (Twomey, 1974) and lifetime (Albrecht,

1989) of clouds. This change in surface radiation is partially balanced by latent heat, leading to changes in precipitation and convection.

Besides the radiative effects, it has been proposed that aerosols can affect convection through purely microphysical pathways. A commonly referenced mechanism (Rosenfeld et al. (2008), see also Williams et al. (2002); Andreae et al. (2004)) posits that increased aerosol concentrations increase cloud droplet number concentrations of smaller drops, which delays the formation of rain. It is thought that this would bring more cloud water above the freezing level, releasing additional latent heat and invigorating convection. Stevens and Feingold (2009) present a liquid variant of this argument, suggesting that the delayed precipitation increases evaporation at the cloud-top, destabilizing the atmosphere and favoring convection. Changes in condensate evaporation can also affect cold pool strength and the strength of subsequent convection (e.g. Tao et al., 2007; Morrison, 2012; Tao et al., 2012). Recently, Fan et al. (2018) suggested that ultrafine (smaller than 50 nm) aerosol particles can be activated into cloud droplets, making it possible to condense more supersaturated water. Given that the enhancement of upper level condensational heating was not significant in their sensitivity tests, they argue that the convective invigoration in their experiments occurs via a warm-phase rather than a cold-phase pathway.

Generally speaking, there is no consensus on how aerosols may affect convection, with different case studies suggesting either strengthening (e.g. Fan et al., 2018) or weakening (e.g. Morrison, 2012). Making comparisons across different case studies is not straightforward, given that environmental factors such as wind shear (e.g. Fan et al., 2009) and radiative effects (e.g. Fan et al., 2015) can alter the eventual convective response. The setting of radiative-convective equilibrium (RCE) allows us to understand which processes are of importance to the climate state in a simple framework. For example, van den Heever et al. (2011) found an increase in the frequency of updrafts in response to increased aerosol concentrations. In a follow-up study focusing on deep convective cloud properties, Storer and van den Heever (2013) showed that changes in latent heat from the freezing of cloud water are not the largest contributors to the latent heat budget, suggesting that latent heat from freezing might not be of leading order importance for understanding convective invigoration, at least in RCE. This motivates a targeted mechanistic study of the importance of ice processes to convective invigoration that eliminates cloud-radiative feedbacks.

2 Methods

2.1 Model

The simulations are performed in RCE using the Advanced Research Weather Research and Forecasting (WRF) model (Wang & Sobel, 2011). The simulation domain is doubly periodic and contains 96x96 gridpoints at a horizontal resolution of 2 km, with fifty vertical levels. Radiative cooling is prescribed at -1.5 K day^{-1} in the troposphere (T $>$ 207.5 K); above 207.5 K, the cooling follows Newtonian relaxation to 200 K on a time scale of 5 days. Prescribing the radiative cooling eliminates a major confounding factor of aerosol-radiation interactions on the convective response. Surface sensible and latent heat fluxes are computed with an aerodynamic formulation following Chua et al. (2019), with surface temperatures set to 28°C. Subgrid diffusion is calculated by the Smagorinsky and YSU (Hong et al., 2006) schemes. Domain-mean winds are nudged to zero on a timescale of two hours. The configuration is identical to that of Chua et al. (2019) except for the use of the double-moment Morrison scheme (Morrison et al., 2009). By predicting both the number and mass mixing ratio of hydrometeors, a double moment scheme captures more degrees of freedom of the microphysical response to aerosols.

The Morrison scheme can be set to only consider liquid (or warm rain) microphysics. In that configuration, condensation of water vapor (q_v) to cloud water (q_c) takes place via saturation adjustment. Re-evaporation of cloud droplets occurs only in subsaturated conditions, and is limited by the availability of cloud water. Rain (q_r) is converted to vapor by rain re-evaporation. The conversion of cloud water to rain occurs by both autoconversion and accretion, parameterized respectively as $1350 q_c^{2.47} N_d^{-1.79}$ and $67(q_c q_r)^{1.15}$, with units of kg kg^{-1} s^{-1} (Khairoutdinov & Kogan, 2000). Here, q_c and q_r are in kg kg^{-1} and N_d is in cm^{-3}. Autoconversion is the only microphysical process among both ice and liquid processes that is directly affected by N_d.

2.2 Experiments

Four pairs of BASE (N_d = 100 cm^{-3}) and BASE* (N_d = 1000 cm^{-3}) simulations are performed with different microphysical assumptions. In FULL, the default Morrison scheme configuration is used, with full ice and liquid microphysics, while LIQ involves only liquid microphysics. In addition to shutting off ice microphysics, the formula used for computing the rates of re-evaporation of cloud water and rain are multiplied by 0.1

in the CE and RE experiments, respectively. We collectively refer to LIQ, CE and RE as liquid microphysics cases. The BASE simulations are initialized from a warm bubble and are first performed for 240 model days. The output at day 180 of the BASE experiment is used to initialize a 60-day-long BASE* experiment. We analyze the last 20 days of hourly-mean output from each simulation. The noise level of a given variable is quantified using five consecutive, non-overlapping 20 day periods (days 220-320) obtained by extending the BASE simulations. The response to higher droplet number concentration (i.e., BASE* minus BASE) is denoted by a δ.

3 Domain-mean vertical responses

Here, we describe the responses of key microphysical, dynamic and thermodynamic quantities to the perturbations imposed by our experiments. In all BASE cases, the distribution of cloud water (q_c, Figure 1a) is similar in the lower and middle troposphere, peaking around 900 hPa. In the upper troposphere, the high clouds are comprised by ice (dashed) in FULL and cloud water in the liquid microphysics cases. Cloud water is larger in FULL than in the liquid microphysics cases. The distribution of precipitating condensates (q_p, Figure 1b) is similar in the lower troposphere across experiments, with a peak at around 700 hPa. Above 600 hPa, the solid condensates (snow and graupel) dominate the precipitating condensates in FULL (dashed). Both q_c and q_p are highest in FULL. In all δBASE* cases (Figure 1e), there is an increase in cloud condensate below 500 hPa. There is also a decrease in q_p below 700 hPa (Figure 1f). The increased cloud water and reduced rain concentrations are consistent with the nature of the perturbation, which suppresses the conversion of cloud water to rain.

Next, we turn to the influence of the microphysical perturbations on convective dynamics. Across the BASE cases, the convective mass flux (M_c, Figure 1c) is largest in FULL. Convective mass flux is the sum of the mass flux from gridpoints where $q_c > 0.005$ g kg^{-1} (e.g. Wang & Sobel, 2011) and vertical velocity exceeds 1 m s^{-1} (e.g. Robe & Emanuel, 1996). Note that convection remains unaggregated across all simulations. Convective invigoration is seen in both FULL and LIQ in δBASE* (Figure 1g), with the peak of the increase in M_c at around 600 hPa, implying that the presence of ice microphysics does not qualitatively alter the convective invigoration response. Relative to LIQ, weakening re-evaporation of cloud droplets (CE) mutes the increase of M_c by 56% at 600 hPa,

while weakening re-evaporation (RE) does not significantly alter convective mass flux below 600 hPa. The increases in M_c at 600 hPa coincide with the increase of q_c.

One might expect the thermodynamic environment to be important for understanding the convective response. Figure 1d shows the relative humidity (RH) in the BASE cases. The profiles exhibit a C-shape, with minima in the mid-troposphere (around 500 hPa). Across the cases, experiments with larger RH generally have larger M_c (Figure 1c, g). The convective invigoration seen in the δBASE* cases coincide with an increase in mid-tropospheric (e.g. 600 hPa) RH (Figure 1h). Having identified that convective invigoration occurs in δBASE* together with increase in mid-tropospheric RH, even in the absence of ice microphysics, we proceed with more quantitative analysis of the connections between the different domain-mean quantities.

4 Connections between thermodynamic, dynamic, and microphysical variables

Figure 2 summarizes the key relationships discussed in Section 3. Comparing across the BASE (circles) and BASE* (asterisks) cases, there is a general correspondence between column relative humidity (CRH) and vertically-averaged convective mass flux [M_c] (Figure 2a). The mid-tropospheric (400 to 600 hPa) relative humidity (MRH) has a monotonic relationship with [M_c] across all cases (Figure 2b). In this sense, the convective invigoration, as well as changes in M_c across the BASE cases, are linked to a increased RH, especially in the mid-troposphere. One way to connect RH to the microphysical perturbation is by considering the ratio of column-integrated re-evaporation (E) to condensation (C), which we denote by γ. Larger values of γ favor larger values of RH in an analytical model of RH which regards re-evaporation as a moistening of the environment (Romps, 2014). Indeed, there is a monotonic relationship between γ and CRH across our simulations (Figure 2c). Increases in γ can also be associated with increases in MRH (Figure 2d).

Table 1 presents the decomposition of γ into E and C, together with other relevant quantities in the microphysical budgets. By definition, changes in $C-E$ must equal changes in P, which changes little (less than 10%) across experiments due to the fixed tropospheric radiative cooling. The assumption of fixed P implies that increases in E increase both C and γ. Relative to LIQ, E is mainly reduced via the weakening of rain and cloud evaporation in RE and CE, respectively. The weakening of EC in CE (26%)

Table 1. The values of γ [the ratio of column-integrated re-evaporation (E) to column-integrated condensation (C)], E and its rain (ER) and cloud (EC) components, C, accretion (AR), precipitation P in the BASE liquid microphysics experiments, and their changes in BASE* (δBASE*). Except for γ, which is unitless, all the quantities are domain-averaged and in mm day^{-1}. The connections between the processes in LIQ are illustrated in Figure 3. In FULL, additional ice processes (Table S1) are involved in ER, EC, C, and AR.

EXPT	γ	E	ER	EC	C	AR	P
BASE							
FULL	0.67	9.1	3.7	5.4	13.7	8.2	4.5
LIQ	0.56	5.8	2.7	3.1	10.2	7.1	4.5
RE	0.37	2.8	0.5	2.3	7.6	5.2	4.7
CE	0.51	4.6	2.7	2.0	9.1	7.1	4.4
δBASE*							
FULL	0.02	0.8	-0.7	1.5	0.9	-0.6	0.1
LIQ	0.04	1.0	-0.6	1.6	1.1	-0.5	0.1
RE	0.09	1.3	-0.2	1.4	1.3	-0.1	0.1
CE	0.02	0.5	-0.6	1.1	0.5	-0.6	0.0

is small compared to the weakening of ER by RE (81%), suggesting that EC is strongly limited by the availability of condensate. To better understand how the increase in E is achieved under a suppression of autoconversion, we investigate the processes underlying the changes in its precipitation (ER) and cloud (EC) re-evaporation components.

Since ice microphysics do not fundamentally alter convective invigoration, we will focus on LIQ (Figure 3a), where the processes are rain (ER) and cloud evaporation (EC), droplet condensation (C), accretion (AR) and autoconversion (CR). In equilibrium, surface evaporation (ES) and precipitation (P) are in balance, as are the sources and sinks of the microphysical terms. One observation is that the conversion of q_c to q_p is mostly from accretion, as one might expect from cloud-resolving simulations (e.g. Heikenfeld et al., 2019) and observations (e.g. Gettelman et al., 2013). This does not mean that autoconversion can be disregarded, because in the absence of q_p and ice microphysics, autoconversion is the only way cloud condensates can be converted to precipitation.

Indeed, a reduction in autoconversion acts to reduce the conversion of cloud to precipitating condensates via accretion (Figure 3b). The reduction in accretion is balanced by a reduction in rain re-evaporation so as to balance the sources and sinks of q_p. To balance the q_c budget, there is a net increase in $EC-C$, which occurs via increases in both EC and C. In other words, the suppression of accretion leads to opposing responses in EC and ER, which act to moisten and dry the atmosphere, respectively, with the former winning out.

The competing effects of EC and ER shed some light on the response across the δBASE* experiments. As in δLIQ*, the other δBASE* experiments exhibit decreases in AR and ER, and increases in E, EC, and C (Table 1). In RE, where the drying response of ER is suppressed, the increase in E is the largest among the δBASE* experiments. In contrast, in CE, the moistening response of EC is suppressed, reducing the increase in E. So far, we have seen that larger values of E increase γ, which is associated with column relative humidity and M_c. In the case of suppressed autoconversion, the increase of cloud re-evaporation exceeds the decrease in rain re-evaporation, leading to a net increase in E. Next, we seek a better understanding of how the changes in microphysical processes influence convective dynamics.

We examine the energy budget (Figure 4) to identify the leading processes responsible for the altered energy transport due to the increases in convective mass flux. In all the BASE cases (a-d), the prescribed radiative cooling (rad) is balanced by latent heating from the microphysics scheme (mp), vertical diffusion in the boundary layer (vdif), and transport of energy by vertical advection from resolved motions (adv). In δBASE*, the changes are largely a compensation between the mp and adv terms. The column-averaged value of the absolute change in the mp term is each case is given in the top left corner of Figure 4e-h. This compensation is similar (within 15%) of the FULL case in LIQ and RE, but is reduced by 44% in CE, consistent with the muting of convective invigoration in CE*. A feature of this compensation is a dipole structure between 800 and 400 hPa, with microphysical heating underneath microphysical cooling that is balanced by advective cooling underneath advective heating. As such, we can think of the convective invigoration as a response to the vertical heating dipole imposed by the microphysical changes.

To understand how the vertical dipole is created in terms of microphysical tendencies, we examine the changes in the latent heat budget (Figure 5). In all the BASE cases, condensation of cloud droplets (cc) peaks lower in the atmosphere (around 900 hPa) than the re-evaporation of cloud and rain condensates (ec and er, respectively). Conceptually, the condensation at cloud base generates buoyancy for the air parcel. As the parcel rises, it detrains cloud condensates, which evaporate into the surrounding air. Across the BASE cases (Figure 5a-d), larger values of γ (e.g. from RE to LIQ) are generally associated with a larger dipole of condensational heating below re-evaporative cooling. In δBASE* (Figure 5e-h), a similar dipole of latent heating beneath cooling is seen. The dipole is mainly a cancellation between condensation (cc) and re-evaporation (ce) of cloud droplets, with ice processes (ice) playing a secondary role. The importance of mid-tropospheric evaporative cooling in creating this latent heating dipole, which we have seen is connected to the changes in convection (Figure 4), is consistent with the monotonic relationship between mid-tropospheric relative humidity and M_c (Figure 2b).

5 Discussion and Conclusions

In interpreting our results, it is useful to return to the microphysical budget constraints (Figure 3). Our perturbation experiments suppress the conversion of cloud condensates to precipitating condensates, giving rise to a reduction in precipitation re-evaporation and a decrease in the net production of cloud condensates. The latter can occur in one of three possible pathways: (1) an increase in condensation and a larger increase in cloud re-evaporation; (2) a decrease in condensation and a smaller (less negative) decrease in cloud re-evaporation; (3) changes in condensation and cloud re-evaporation that differ in sign (e.g. an increase in cloud re-evaporation and a decrease in condensation). Pathway (2) does not occur because the suppressed accretion increases the concentration of cloud condensates, which seems to be the factor limiting cloud re-evaporation. For example, if one contrasts CE with LIQ, despite the prescribed 10-fold decrease in the parameterization, the actual cloud re-evaporation decreases by only 26%. It is reasonable to assume that condensation and cloud re-evaporation tend to change in the same direction. This is borne out in our simulations (Table 1), and allows us to rule out (3).

A plausible explanation for convective invigoration in the context of liquid or warm rain microphysics is then as follows. Increased cloud droplet number concentrations reduce accretion via the suppression of autoconversion. In the dry mid-troposphere, cloud

re-evaporation is limited by condensate availability. Hence, the increased cloud condensates (due to weaker accretion) act to increase cloud re-evaporation. The additional re-evaporative cooling is balanced by more condensational heating lower in the atmosphere (Figure 5), creating a dipole that dynamically further enhances condensation and convective mass flux. Since precipitation is fixed, the increase in condensation must be accompanied by an increase in total re-evaporation (from cloud and precipitating condensates combined), which also favors condensation by moistening the mid-troposphere. Note that this argument is consistent with (i) the increase in cloud re-evaporation outweighing the decrease in precipitation re-evaporation and (ii) the relationship between mid-tropospheric relative humidity and convective mass flux (Figure 2b).

A contemporaneous study by Abbott and Cronin (2020) allows us to examine the robustness of our results to the choice of model configuration and N_d. Both studies find that an increase in N_d gives rise to increased mid-tropospheric relative humidity in RCE and convective invigoration, even in the absence of ice microphysics. We examine convective invigoration via convective mass flux in RCE, whereas their study focuses on changes in high-percentile vertical velocities under the assumption of weak temperature gradient (WTG) balance.

Ice microphysical processes are often thought to play a key role in enhancing convection under polluted conditions (convective invigoration). In the setting of radiative-convective equilibrium with prescribed radiative cooling, we demonstrate that an increase in cloud droplet number concentration can cause an increase in convective mass flux even in the absence of ice microphysical processes. Subsequent sensitivity tests of liquid microphysical processes indicate that this convective invigoration depends more strongly on cloud re-evaporation as opposed to rain re-evaporation. A microphysical process analysis reveals that the increased cloud droplet number concentrations reduces the rate of conversion of cloud water to rain and leads to an increase in cloud re-evaporation and a decrease in precipitation re-evaporation, with the former outweighing the latter. Suppressing cloud (rain) re-evaporation weakens the responses in cloud (rain) re-evaporation. Besides increasing the relative humidity, the increase in re-evaporation helps create a dipole of condensational heating beneath re-evaporative cooling, with an associated increase in convective mass flux.

Acknowledgments

We are very grateful to Shuguang Wang for providing the source code for the version of WRF used in this study, and the developers of the "aospy" package. XRC was funded by the Cooperative Institute for Climate Science and the Singapore National Research Foundation. We thank Tristan Abbott, Tim Cronin, Nadir Jeevanjee and Hugh Morrison for helpful discussions, and appreciate guidance in the early stages by Hailey Shin, Usama Anber, and Spencer Clark. We appreciate the thoughtful comments by Ming Zhao and the reviewers.

References

Albrecht, B. A. (1989, Sep 15). Aerosols, cloud microphysics, and fractional cloudiness. *Science*, *245*(4923), 1227.

Andreae, M. O., Rosenfeld, D., Artaxo, P., Costa, A. A., Frank, G. P., Longo, K. M., & Silva-Dias, M. A. F. (2004). Smoking rain clouds over the Amazon. *Science*, *303*(5662), 1337–1342.

Chua, X. R., Ming, Y., & Jeevanjee, N. (2019). Investigating the fast response of precipitation intensity and boundary layer temperature to atmospheric heating using a cloud-resolving model. *Geophysical Research Letters*, *46*(15), 9183-9192. Retrieved from `https://agupubs.onlinelibrary.wiley.com/doi/abs/10.1029/2019GL082408` doi: 10.1029/2019GL082408

Fan, J., Rosenfeld, D., Yang, Y., Zhao, C., Leung, L. R., & Li, Z. (2015). Substantial contribution of anthropogenic air pollution to catastrophic floods in Southwest China. *Geophysical Research Letters*, *42*(14), 6066–6075.

Fan, J., Rosenfeld, D., Zhang, Y., Giangrande, S. E., Li, Z., Machado, L. A., ... others (2018). Substantial convection and precipitation enhancements by ultrafine aerosol particles. *Science*, *359*(6374), 411–418.

Fan, J., Yuan, T., Comstock, J. M., Ghan, S., Khain, A., Leung, L. R., ... Ovchinnikov, M. (2009). Dominant role by vertical wind shear in regulating aerosol effects on deep convective clouds. *Journal of Geophysical Research: Atmospheres*, *114*(D22).

Gettelman, A., Morrison, H., Terai, C., & Wood, R. (2013). Microphysical process rates and global aerosol-cloud interactions. *Atmospheric Chemistry and Physics*, *13*(19), 9855–9867.

Heikenfeld, M., White, B., Labbouz, L., & Stier, P. (2019). Aerosol effects on deep convection: the propagation of aerosol perturbations through convective cloud microphysics. *Atmospheric Chemistry and Physics*, *19*(4), 2601–2627.

Hong, S.-Y., Noh, Y., & Dudhia, J. (2006). A new vertical diffusion package with an explicit treatment of entrainment processes. *Monthly Weather Review*, *134*(9), 2318–2341.

Khairoutdinov, M., & Kogan, Y. (2000). A new cloud physics parameterization in a large-eddy simulation model of marine stratocumulus. *Monthly Weather Review*, *128*(1), 229–243.

Morrison, H. (2012). On the robustness of aerosol effects on an idealized supercell storm simulated with a cloud system-resolving model. *Atmospheric Chemistry and Physics*, *12*(16), 7689–7705.

Morrison, H., Thompson, G., & Tatarskii, V. (2009). Impact of cloud microphysics on the development of trailing stratiform precipitation in a simulated squall line: Comparison of one-and two-moment schemes. *Monthly Weather Review*, *137*(3), 991–1007.

Robe, F. R., & Emanuel, K. A. (1996). Moist convective scaling: Some inferences from three-dimensional cloud ensemble simulations. *Journal of the Atmospheric Sciences*, *53*(22), 3265–3275.

Romps, D. M. (2014). An analytical model for tropical relative humidity. *Journal of Climate*, *27*(19), 7432–7449.

Rosenfeld, D., Lohmann, U., Raga, G. B., O'Dowd, C. D., Kulmala, M., Fuzzi, S., ... Andreae, M. O. (2008). Flood or drought: how do aerosols affect precipitation? *Science*, *321*(5894), 1309–1313.

Stevens, B., & Feingold, G. (2009). Untangling aerosol effects on clouds and precipitation in a buffered system. *Nature*, *461*(7264), 607.

Storer, R. L., & van den Heever, S. C. (2013). Microphysical processes evident in aerosol forcing of tropical deep convective clouds. *Journal of the Atmospheric Sciences*, *70*(2), 430–446.

Tao, W.-K., Chen, J.-P., Li, Z., Wang, C., & Zhang, C. (2012). Impact of aerosols on convective clouds and precipitation. *Reviews of Geophysics*, *50*(2).

Tao, W.-K., Li, X., Khain, A., Matsui, T., Lang, S., & Simpson, J. (2007). Role of atmospheric aerosol concentration on deep convective precipitation: Cloud-

resolving model simulations. *Journal of Geophysical Research: Atmospheres*, *112*(D24).

Twomey, S. (1974). Pollution and the planetary albedo. *Atmospheric Environment*, *8*(12), 1251–1256.

van den Heever, S. C., Stephens, G. L., & Wood, N. B. (2011). Aerosol indirect effects on tropical convection characteristics under conditions of radiative–convective equilibrium. *Journal of the Atmospheric Sciences*, *68*(4), 699–718.

Wang, S., & Sobel, A. H. (2011). Response of convection to relative sea surface temperature: Cloud-resolving simulations in two and three dimensions. *Journal of Geophysical Research: Atmospheres*, *116*(D11).

Williams, E., Rosenfeld, D., Madden, N., Gerlach, J., Gears, N., Atkinson, L., ... others (2002). Contrasting convective regimes over the Amazon: Implications for cloud electrification. *Journal of Geophysical Research: Atmospheres*, *107*(D20), LBA–50.

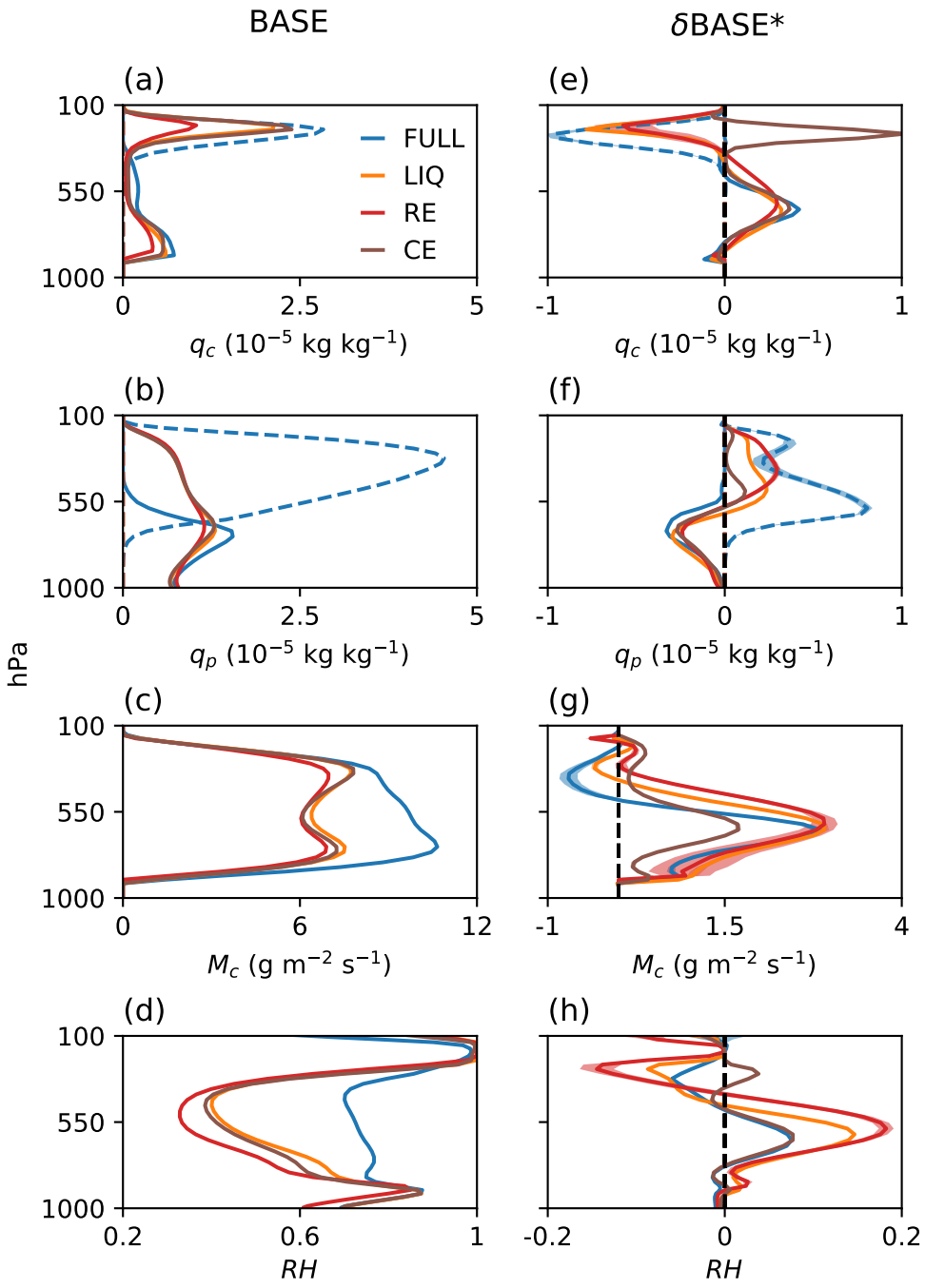

Figure 1. Domain-average vertical profiles of (a) cloud liquid (solid) and ice (dashed) condensates (q_c, 10^{-5} kg kg^{-1}), (b) precipitating liquid (solid) and ice (dashed) condensates (q_p, 10^{-5} kg kg^{-1}), (c) convective mass flux (M_c, g m^{-2} s^{-1}) (d) relative humidity (RH, unitless), (e-h) Changes in (a-d) due to δBASE*. The shading in (e-h) represents the noise in BASE.

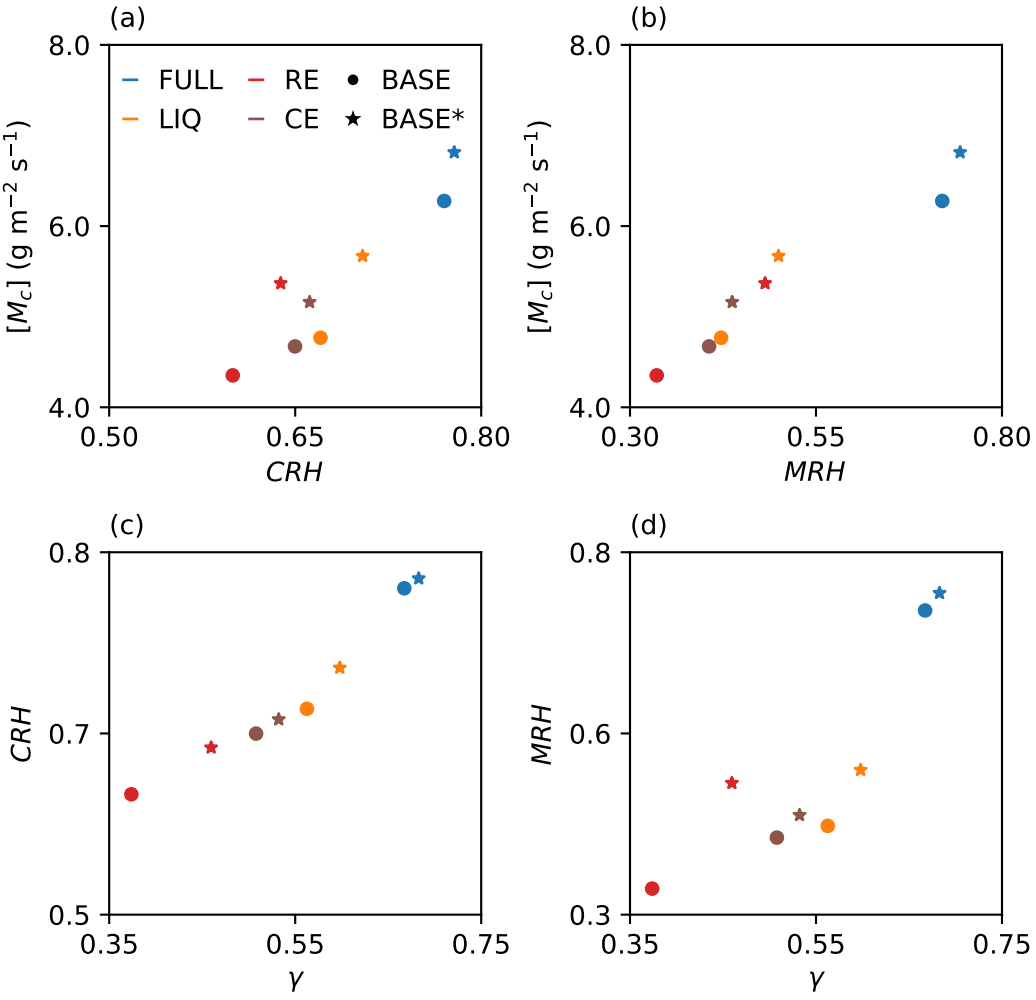

Figure 2. Scatter plots of (a) vertically averaged convective mass flux ($[M_c]$, g m^{-2} s^{-1}) against column relative humidity (CRH), (b) $[M_c]$ against mid-tropospheric (600 to 400 hPa) relative humidity (MRH), (c) CRH against the ratio of column-integrated re-evaporation to condensation (γ, unitless), (d) MRH against γ in all experiments.

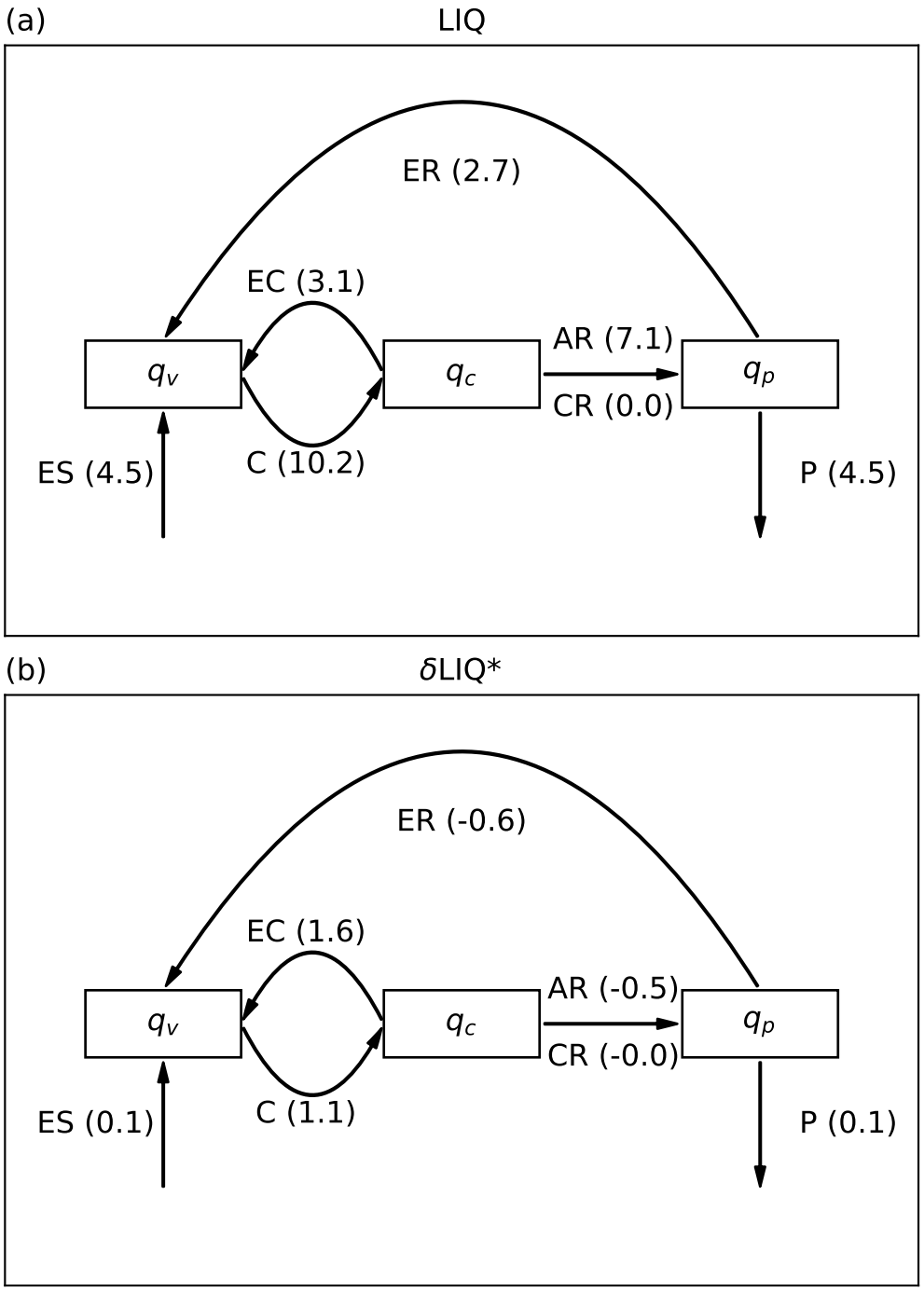

Figure 3. Column-integrated and domain-averaged values (mm day^{-1}) of microphysical processes converting between water vapor (q_v), cloud condensates (q_c) and precipitating condensates (q_p) [condensation of cloud condensates (C), evaporation of cloud condensates (EC), conversion of cloud water to rain by autoconversion (CR) and accretion (AR) and evaporation of rain (ER)], as well as surface evaporation (ES) and precipitation (P) for (a) LIQ and (b) δLIQ*. The corresponding values for all configurations are listed in Table 1.

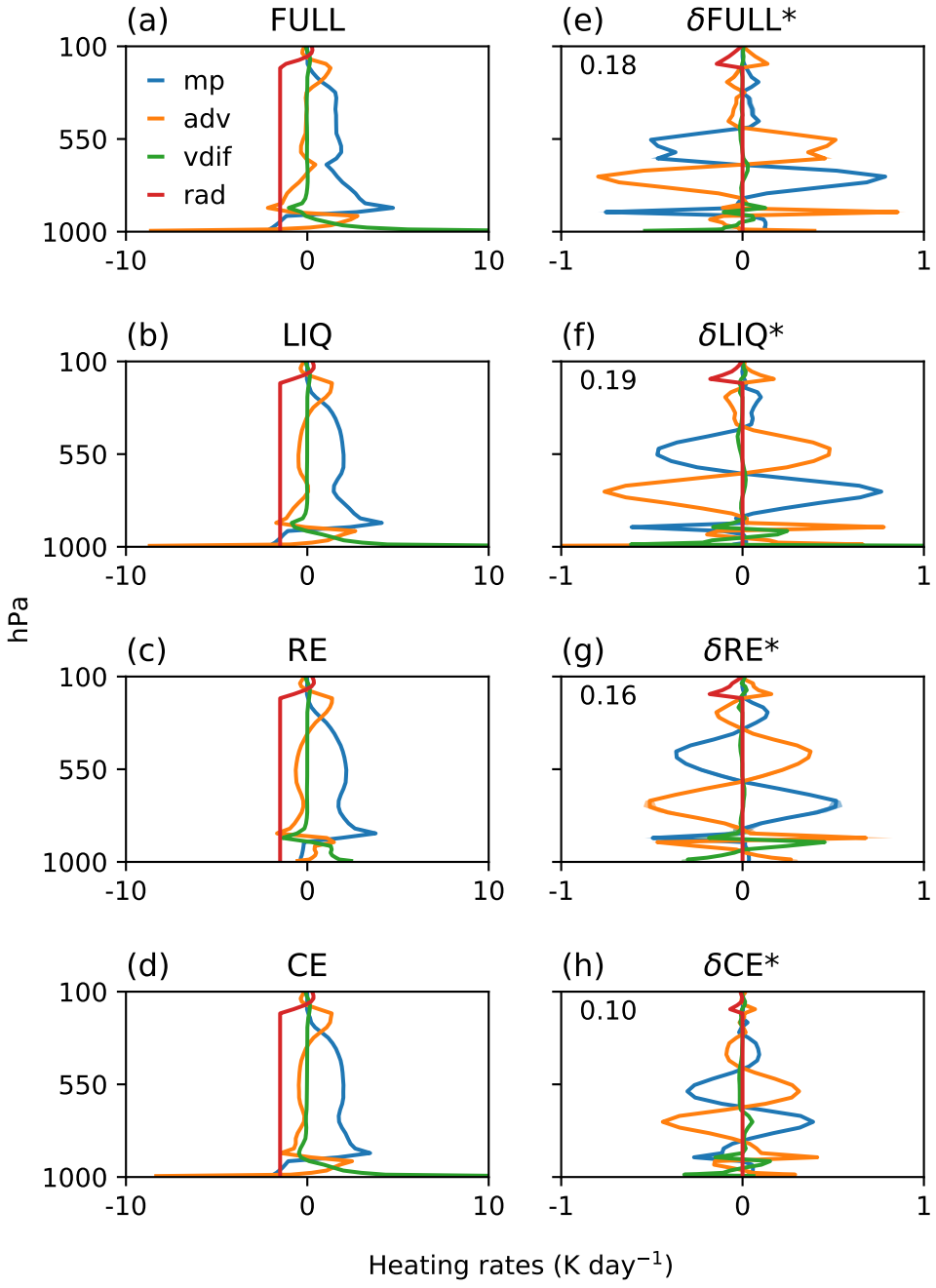

Figure 4. Domain-average vertical profiles of the microphysical (mp), advection (adv), vertical diffusion (vdif) and radiative (rad) heating rates in (a) FULL, (b) LIQ, (c) RE and (d) CE. (e-h) Changes in (a-d) due to δBASE*. The vertically-averaged value of the absolute changes in mp is given on the top left hand corner. All values are in K day^{-1}.

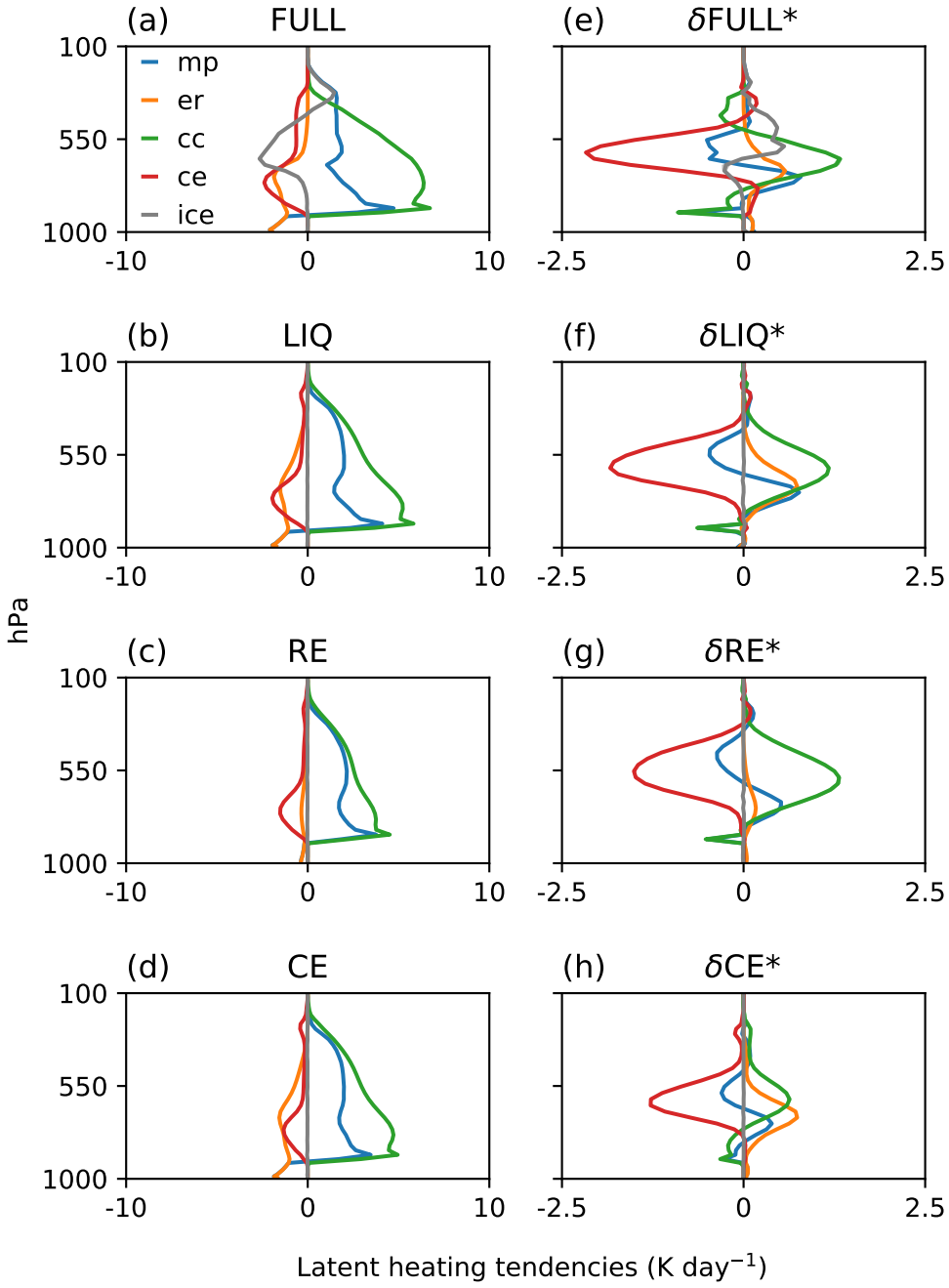

Figure 5. The decomposition of the microphysical term in Figure 4 (mp) into contributions from rain re-evaporation (er), formation of cloud droplets by condensation (cc), evaporation of cloud droplets (ec), and ice processes (ice) in the BASE configurations (a) FULL, (b) LIQ, (c) RE and (d) CE. (e-h) Changes in (a-d) due to δBASE*. All values are in K day^{-1}.